



PCCP

Local electronic structure of histidine in aqueous solution

Journal:	<i>Physical Chemistry Chemical Physics</i>
Manuscript ID	CP-ART-01-2021-000361.R1
Article Type:	Paper
Date Submitted by the Author:	03-Mar-2021
Complete List of Authors:	Kostko, Oleg; Lawrence Berkeley National Laboratory, Chemical Sciences Division Xu, Bo; Lawrence Berkeley National Laboratory, Chemical Sciences Division Ahmed, Musahid; Lawrence Berkeley National Laboratory, Chemical Sciences Division

SCHOLARONE™
Manuscripts

1 **Local electronic structure of histidine in aqueous solution**

2 O. Kostko,^{1,2,a)} B. Xu,¹ and M. Ahmed¹

3 ¹ Chemical Sciences Division, Lawrence Berkeley National Laboratory, Berkeley, CA 94720, USA

4 ² Advanced Light Source, Lawrence Berkeley National Laboratory, Berkeley, CA 94720, USA

5 a) Electronic mail: OKostko@lbl.gov

6

7 **ABSTRACT**

8 The local electronic structure of aqueous histidine, an amino acid important in nature and biology, is
9 revealed by aerosol X-ray photoemission spectroscopy. A detailed picture of the photoionization
10 dynamics emerges by tuning the pH of the aqueous solution from which the aerosols are generated
11 allowing us to report the X-ray photoelectron spectroscopy (XPS) of histidine. Assignment of the
12 experimental photoelectron spectra of the C1s and N1s levels allows for determination of the
13 protonation state of histidine in these aqueous aerosols and is confirmed by density functional
14 calculations. XPS spectra show that at pH = 1, both imidazole and amine group nitrogens are protonated,
15 at pH = 7, the amine group nitrogen is protonated and carboxyl group carbon is deprotonated resulting
16 in zwitterionic structure and at pH = 13, only the carboxyl group remains deprotonated. Comparison of
17 these results with previous experimental and theoretical results suggests that X-ray spectroscopy on
18 aqueous aerosols can provide a convenient and simple way of probing electronic structure in aqueous
19 solutions.

20 INTRODUCTION

21 Amino acids constitute the elementary building blocks of proteins, are metabolic intermediates,
22 and play important roles in living organisms. To advance our understanding of their roles and functions
23 in biology, it is important to determine the electronic and geometric structure of amino acids
24 particularly in a solvent environment such as water. X-ray spectroscopic techniques are powerful tools
25 for investigations of electronic structure of matter and have been extensively applied to amino acids.
26 However, most of these investigations have been restricted to solid state¹⁻⁸ or the gas phase amino
27 acids⁹⁻¹² while biochemical systems almost universally occur in aqueous environment. In the gas phase,
28 amino acids exclusively exist in the neutral (molecular) form,¹³⁻¹⁵ and they are zwitterionic in the
29 condensed phase.¹⁶ In biologically relevant aqueous environments, amino acids exist in a wide variety of
30 charge states whose relative populations are determined by the pH of the solution. Amino acids exist as
31 a cation in acidic media with its amine group protonated, whereas the carboxyl group is neutral. For a
32 basic solution, the amine and carboxyl groups are both deprotonated and the amino acid acts as an
33 anion. For intermediate pH values, amino acids form a zwitterionic state, leading to an overall charge-
34 neutral state.

35 Histidine is an amino acid with an imidazole ring side chain, the charge state of which depends on
36 the environmental pH (Fig. 1).¹⁷⁻¹⁹ Because of its pH-dependent protonation, histidine is involved in the
37 functions of proteins²⁰ and plays a very important role in proton conduction,²¹ enzyme catalysis,²² and
38 metal-requiring enzymes.²³ From the viewpoint of molecular assembly in synthetic biology, amino acids
39 and peptides can play very important roles due to their side chains,^{24,25} and in the case of histidine, the
40 possibility of the imidazole motif to π -stack and act as nucleation sites. Recently, we demonstrated a
41 self-assembly process in arginine-oleic acid solutions, which is pH dependent leading to the formation of
42 micelles, vesicles and finally sponges in basic medium.²⁶ In histidine derived peptides, liquid-liquid phase
43 separations have been invoked to give rise to the formation of hydrogels or coacervate micro-droplets
44 which are also pH dependent.²⁷ The imidazole motif prevalent in histidine has also been implicated in
45 nucleation and crystallization processes in concentrated aqueous media, however neutron diffraction
46 and X-ray scattering studies suggest that it is solvation which drives assembly and not π -stacking of the
47 imidazole pairs.²⁸

48 Several X-ray absorption,^{29,30} X-ray emission,³¹ and resonant inelastic X-ray scattering (RIXS)^{32,33}
49 studies have been conducted on glycine, proline, cysteine, and lysine to investigate the change of their
50 electronic structures engendered by varying the pH of solutions. The above mentioned techniques
51 provide a view of the bulk solution, while X-ray photoelectron spectroscopy (XPS), which can provide
52 direct information on electronic structure of the surface and interface, brings an extra layer of sensitivity
53 to the measurements. However only recently has it been applied for the study of highly volatile aqueous
54 solutions via liquid jet³⁴ technology, to probe the electronic structure of lysine,³⁵ glycine,³⁶ and
55 imidazole³⁷ (the side chain of histidine), while we have pioneered the use of aqueous aerosols to
56 investigate arginine with XPS³⁸ and valence band spectroscopy.³⁹ The XPS studies revealed large spectral
57 energy shifts of the N1s and C1s photoemission peaks as a function of pH, showing it has a large
58 influence on the electronic structure of amino acids.

59 While the solution phase pH dependence has been probed by vibrational spectroscopy⁴⁰ and NMR
60 methods,¹⁷ most of X-ray studies to date have focused on solid state histidine. XPS^{8,41,42} and near-edge
61 X-ray absorption fine structure (NEXAFS)^{2,43} measurements of solid histidine and other biomolecules
62 were supported by theoretical investigation of NEXAFS spectra of amino acids.⁴⁴ A recent publication
63 discusses NEXAFS and RIXS of histidine's N K-edge in aqueous solution at basic, neutral, and acidic
64 conditions.⁴⁵ In the present work, we report on the impact of the pH variation on the local electronic
65 structure of histidine in solution using XPS applied to the aqueous aerosols combined with theory. We
66 demonstrate that we can extract protonation states of both carbon and nitrogen atoms at various pH
67 conditions revealing valuable information for small biomolecules.

68 METHODS

69 Histidine was obtained commercially from Sigma-Aldrich (purity above 99%) and used without
70 further purification. Initial 0.1 mol/L amino acid solutions were prepared with highly demineralized
71 water. pH values of 1.0, 7.0, and 13.0 (± 0.2) were adjusted either with hydrochloric acid or sodium
72 hydroxide.

73 In this study, a velocity map imaging (VMI) spectrometer combined with an aerodynamic lens^{38,46}
74 was used to obtain the XPS of histidine aqueous aerosol nanoparticles. Aqueous aerosol nanoparticles
75 were generated by atomizing 0.1 mol/L histidine aqueous solution via a high flux atomizer (Model 3076,
76 TSI). Dry nitrogen is used as carrier gas for the C1s level while oxygen is used for the N1s level
77 measurements. The size distribution of the nanoparticles is measured with a commercial scanning
78 mobility particle sizer (SMPS, TSI). This distribution is broad with a mean particle diameter of 170 nm
79 (surface to volume ratio of 3.7%), providing a nanoscaled solution environment. After passing through a
80 set of aerodynamic lenses, the nanoparticles are tightly focused to a beam. The beam diameter is 1 mm
81 with a computed flux of 10^7 particles/s at the interaction region. The photon beam generated by the
82 beamline 11.0.2 at the Advanced Light Source, Lawrence Berkeley National Laboratory intersects the
83 nanoparticle beam orthogonally and leads to photoemission.

84 Typical accumulation times for a photoelectron image is about 15 minutes. A background image is
85 collected with an inline filter inserted, which removes all of the nanoparticles from the beam and is
86 subtracted from the data image. The velocity distributions from the background-subtracted
87 reconstructed images is performed using the pBASEX algorithm.⁴⁷ The spectrometer is calibrated with
88 N1s spectra of N₂, in order to relate radial position in the image to electron kinetic energy (KE). C1s and
89 N1s spectra presented in the paper are obtained by subtracting a linear background from raw data. The
90 photon energy was calibrated by measuring XPS of nitrogen gas at 425 eV, and the obtained binding
91 energy of N1s is 409.9 eV. Electron binding energies (BE) reported here are with respect to vacuum.
92 Throughout this paper, when molecular formula fragments are reported, the atom of interest is
93 indicated by being underlined where there is possible ambiguity.

94 Theoretical photoelectron spectra are calculated using the Gaussian 09 computational chemistry
95 package to help assignment of experimental XPS data.⁴⁸ Geometrical structures of histidine molecules
96 are optimized using ω B97X-D functional with a 6-311+g(d,p) basis set in the presence of solvent
97 simulated by the polarizable continuum model (PCM). The XPS peak positions and corresponding
98 chemical shifts are obtained using Koopmans' theorem (also known as "initial state") approximation for

99 the density functional theory.⁴⁹ According to the approximation, the final state effects are neglected and
100 electron BEs and corresponding BE shifts are found only for initial state of the molecule. While the
101 method is not very accurate for finding absolute values of BEs, it is rather precise and widely used to
102 predict BE shifts. Calculated values of binding energies are blue shifted by 9.3 eV for C1s and by 10.9 eV
103 for N1s electrons to correlate with experimental data for histidine solution with pH = 7.

104 RESULTS AND DISCUSSION

105 Photoelectron spectra of aqueous solutions of histidine at three different pH values are shown in
106 Fig. 2. XPS spectra of the N1s level are collected using the photon energy of 425 eV, whereas the C1s
107 spectra are collected at photon energy of 310 eV, resulting in kinetic energy of emitted electrons of 20
108 eV. While the shape of C1s spectra at three different pH values are very similar, the N1s spectrum
109 becomes broader with the increase of pH, but the common trend is that both N1s and C1s peaks shift to
110 lower binding energy with the increase of pH. That is due to change of the net histidine charge from +2
111 (cation) at pH = 1, to neutral (the zwitterion form) in neutral solution, to -1 (anion) at pH = 13. The
112 increase of electron density around histidine results in the shift of N1s and C1s peaks to lower BE during
113 the increase of pH.

114 The experimental spectra were fit using Gaussian functions with fixed FWHM of 1.5 eV in such a
115 way, that the sum of peak areas reflects expected stoichiometric ratios for the chemical environments
116 within the histidine molecule (Fig. 1) and are presented in Table 1. A building block approach, based on
117 literature data on XPS of aqueous solutions of glycine,^{36,38} arginine,³⁸ and imidazole³⁷ was used to assign
118 the collected experimental data.

119 At pH = 1, the peak with the highest binding energy of 406.6 eV could be assigned as the amine
120 group (NH₃⁺) nitrogen (Fig. 2, left panel). The two remaining peaks are due to the imidazole group. Due
121 to protonation of the imidazole group, both N atoms in the group are in a close chemical environment
122 and therefore corresponding N1s peaks lie near each other at binding energies of 406.0 and 405.6 eV.
123 When the pH of the solution is increased to 7, the imidazole group becomes neutral while the amine
124 group remains protonated. Because all three N atoms are in different environments, the three peaks
125 used to fit the experimental data are well separated. The peak corresponding to the unchanged amine
126 group, shifts to slightly lower binding energy of 406.1 eV. Whereas both imidazole N atoms experience
127 stronger BE shifts: the N=C–NH and N=C–NH 1s photoemission lines occur at 405.0 and 403.6 eV,
128 respectively. At pH = 13, both the amine and imidazole groups are deprotonated. The imidazole group
129 maintains the same charge as at pH = 7 and therefore N=C–NH peak stays at 405.0 eV, whereas N=C–NH
130 peak shifts to lower BE of 403.2 eV, separating the imidazole group peaks by 1.8 eV, what is close to the
131 experimental value of 1.7 eV reported for aqueous imidazole.³⁷ In agreement with previous XPS studies
132 of aqueous glycine,^{36,38} deprotonation of the amine group leads to a significant decrease of
133 corresponding N1s BE by 2.0 - 2.5 eV and results in amine's N1s peak of histidine at 403.9 eV.

134 The shape of C1s spectra (Fig. 2, right panel) does not change so strongly as that of the N1s spectra.
135 All three spectra have a shoulder at high BE which is due to the ionization of the carboxyl group and
136 correlates well with the similar peak in glycine.^{36,38} The larger peak in C1s spectra is due to
137 photoemission from the remaining five carbon atoms, which complicates assignment of the individual
138 peaks. The lowest BE component could be due to aliphatic C–C carbon, whereas the two peaks in

139 between of carboxyl and aliphatic carbons should be due to imidazole's and amine's C1s peaks.
140 According to previous XPS data for imidazole³⁷ and glycine,^{36,38} at pH =1 the peak at 291.6 eV is due to
141 the amine group and N=C–NH carbon in the imidazole group. Two remaining imidazole carbons (labeled
142 C–N in Fig. 2) result in a peak at 290.9 eV. Increase of pH to 7 leads to deprotonation of the carboxyl
143 group, which shifts the corresponding peak BE by 0.8 eV, what is less than that observed in glycine (1.0
144 eV³⁶ or 1.1 eV³⁸), but larger than that observed in arginine (0.7 eV³⁸). Deprotonation of the imidazole
145 group and change of net molecule's charge from +2 to 0 leads to decrease of BE of the remaining peaks,
146 but does not change their order. The peak at 290.8 eV is due to glycine's and imidazole's N=C–NH
147 carbons, whereas the peak at 290.0 eV is due to two other imidazole's carbon atoms. Increase of pH to
148 13 leads to deprotonation of the amine group and change of peak order within the large peak in
149 histidine's C1s XPS spectrum (Fig. 2, bottom right panel). The imidazole's N=C–NH carbon appears at BE
150 = 290.5 eV, whereas the amine's carbon (C–NH₂) shifts to BE of 290.0 eV, joining two imidazole's
151 carbons.

152 While the building block's approach allows for a tentative assignment of the XPS spectra, we
153 performed theoretical calculation as outlined above to confirm these assignments and gain further
154 insight into the electronic structure of solvated histidine. To reproduce the experimental spectra, in
155 particular the splitting on carboxyl's carbon it was necessary to explicitly insert four water molecules
156 around histidine molecule as shown in Fig. S1 in Supporting Information. This model at various levels of
157 theory have been implemented in studying the core level shifts in aqueous glycine.^{36,50,51} The calculated
158 spectra, based on binding energies summarized in Table 2, are convoluted with a Gaussian with FWHM =
159 1.2 eV to resemble experimental spectra and are shown in Fig. 3. The calculated spectra reproduce the
160 main features of the experimental XPS spectra. Thus for the N1s peak, one can see that the peak gets
161 broader at pH = 7 and pH = 13, and the asymmetric shape of the peaks at those pH is well reproduced.
162 The theory confirms our assignment with only one major difference: deprotonation of the amine group
163 caused by increase of pH from 7 to 13 leads to decrease of corresponding N1s BE by 3.1 eV instead of
164 the 2.2 eV observed in the experiment, shifting the primary amine's nitrogen from the most bound at pH
165 = 1 and 7 to the least bound at pH = 13. The observed discrepancy with the experiment may arise from
166 the simple level of theory to extract electron BE's, namely Koopmans' theorem. However, the
167 correlation of theory with the experiment is better for C1s spectra, reproducing the predicted
168 assignments and shifts of peaks, such as merged Gaussian peaks of double (at pH =1 and 7) or triple (at
169 pH = 13) intensity. In the future, better theoretical models coupled to a higher level of calculations
170 should provide for a more robust fit to our experimental results.

171 Although we discuss only the π -tautomer of histidine, shown in Figure 1, there is another, τ -
172 tautomer, which has another deprotonated nitrogen in the imidazole moiety.^{17–19} Our DFT calculation
173 revealed that the π -tautomer is energetically favorable over the τ -tautomer by 52 meV at pH = 7 and by
174 25 meV at pH = 13. The computed XPS spectra for both tautomers are presented in Fig. S2 and
175 demonstrate similarity, with one noticeable difference for N1s at pH = 7, where the peak is broader for
176 the τ -tautomer. While the resolution of our experimental spectra does not allow for an unequivocal
177 identification, previous investigations⁴⁵ and energetics would suggest that the π -tautomer is the
178 dominant species.

179 CONCLUSIONS

180 X-ray photoelectron spectra of histidine aqueous aerosols at different pH values were obtained using
181 the velocity map imaging photoelectron spectrometer combined with an aerodynamic lens. Application
182 of a building block approach allowed for identification of the individual nitrogen and carbon atoms of
183 aqueous histidine by their respective core-level binding energies. Electron binding energies, extracted
184 from DFT calculations of the histidine at different pH values of solution confirmed assignment of the
185 experimental spectra. This allowed for identification of protonation states of individual carbon and
186 nitrogen atoms in histidine molecule. This study also demonstrates that velocity map imaging XPS of
187 aqueous aerosols is a powerful technique allowing to probe the electronic structures of biological
188 molecules in their natural aqueous environment.

189 CONFLICTS OF INTEREST

190 There are no conflicts to declare.

191 ACKNOWLEDGEMENTS

192 The authors thank Michael Jacobs for help during setup of the experiment. This work is supported by the
193 Condensed Phase and Interfacial Molecular Science Program, in the Chemical Sciences Geosciences and
194 Biosciences Division of the Office of Basic Energy Sciences of the U.S. Department of Energy under
195 Contract No. DE-AC02-05CH11231. This research used resources of the Advanced Light Source, which is
196 a DOE Office of Science User Facility under Contract No. DE-AC02-05CH11231.

197 REFERENCES

- 198 1 M. Schmidt and S. G. Steinemann, XPS studies of amino acids adsorbed on titanium dioxide surfaces,
199 *Fresenius J. Anal. Chem.*, 1991, **341**, 412–415.
- 200 2 J. Boese, A. Osanna, C. Jacobsen and J. Kirz, Carbon edge XANES spectroscopy of amino acids and
201 peptides, *J. Electron Spectrosc. Relat. Phenom.*, 1997, **85**, 9–15.
- 202 3 J. Hasselström, O. Karis, M. Nyberg, L. G. M. Pettersson, M. Weinelt, N. Wassdahl and A. Nilsson, The
203 Bonding and Electronic Structure Changes upon Adsorption of Important Functional Groups: Glycine
204 on Copper, *J. Phys. Chem. B*, 2000, **104**, 11480–11483.
- 205 4 M. Tanaka, K. Nakagawa, T. Koketsu, A. Agui and A. Yokoya, Oxygen K-edge X-ray absorption near
206 edge structures (XANES) of sublimated films of amino acids, *J. Synchrotron Radiat.*, 2001, **8**, 1009–
207 1011.
- 208 5 K. Kaznatcheyev, A. Osanna, C. Jacobsen, O. Plashkevych, O. Vahtras, Ågren, V. Carravetta and A. P.
209 Hitchcock, Innershell Absorption Spectroscopy of Amino Acids, *J. Phys. Chem. A*, 2002, **106**, 3153–
210 3168.
- 211 6 Y. Zubavichus, A. Shaporenko, M. Grunze and M. Zharnikov, NEXAFS Spectroscopy of
212 Homopolypeptides at All Relevant Absorption Edges: Polyisoleucine, Polytyrosine, and Polyhistidine,
213 *J. Phys. Chem. B*, 2007, **111**, 9803–9807.
- 214 7 C. P. Schwartz, R. J. Saykally and D. Prendergast, An analysis of the NEXAFS spectra of a molecular
215 crystal: α -glycine, *J. Chem. Phys.*, 2010, **133**, 044507.
- 216 8 J. S. Stevens, A. C. de Luca, M. Pelendritis, G. Terenghi, S. Downes and S. L. M. Schroeder,
217 Quantitative analysis of complex amino acids and RGD peptides by X-ray photoelectron spectroscopy
218 (XPS), *Surf. Interface Anal.*, 2013, **45**, 1238–1246.
- 219 9 A. R. Slaughter and M. S. Banna, Core-photoelectron binding energies of gaseous glycine: correlation
220 with its proton affinity and gas-phase acidity, *J. Phys. Chem.*, 1988, **92**, 2165–2167.
- 221 10 I. Powis, E. E. Rennie, U. Hergenbahn, O. Kugeler and R. Bussy-Socrate, Investigation of the Gas-Phase
222 Amino Acid Alanine by Synchrotron Radiation Photoelectron Spectroscopy, *J. Phys. Chem. A*, 2003,
223 **107**, 25–34.
- 224 11 O. Plekan, V. Feyer, R. Richter, M. Coreno, M. de Simone, K. C. Prince and V. Carravetta, Investigation
225 of the Amino Acids Glycine, Proline, and Methionine by Photoemission Spectroscopy, *J. Phys. Chem.*
226 *A*, 2007, **111**, 10998–11005.
- 227 12 O. Plekan, V. Feyer, R. Richter, M. Coreno, M. de Simone, K. C. Prince and V. Carravetta, An X-ray
228 absorption study of glycine, methionine and proline, *J. Electron Spectrosc. Relat. Phenom.*, 2007, **155**,
229 47–53.
- 230 13 W. D. Price, R. A. Jockusch and E. R. Williams, Is Arginine a Zwitterion in the Gas Phase?, *J. Am. Chem.*
231 *Soc.*, 1997, **119**, 11988–11989.
- 232 14 J. Rak, P. Skurski, J. Simons and M. Gutowski, Low-Energy Tautomers and Conformers of Neutral and
233 Protonated Arginine, *J. Am. Chem. Soc.*, 2001, **123**, 11695–11707.
- 234 15 M. Remko and B. M. Rode, Effect of Metal Ions (Li^+ , Na^+ , K^+ , Mg^{2+} , Ca^{2+} , Ni^{2+} , Cu^{2+} , and Zn^{2+}) and
235 Water Coordination on the Structure of Glycine and Zwitterionic Glycine, *J. Phys. Chem. A*, 2006, **110**,
236 1960–1967.
- 237 16 P.-G. Jönsson and Å. Kvik, Precision neutron diffraction structure determination of protein and
238 nucleic acid components. III. The crystal and molecular structure of the amino acid α -glycine, *Acta*
239 *Crystallogr. Sect. B*, 1972, **28**, 1827–1833.
- 240 17 S. Li and M. Hong, Protonation, Tautomerization, and Rotameric Structure of Histidine: A
241 Comprehensive Study by Magic-Angle-Spinning Solid-State NMR, *J. Am. Chem. Soc.*, 2011, **133**, 1534–
242 1544.

- 243 18 M. Munowitz, W. W. Bachovchin, J. Herzfeld, C. M. Dobson and R. G. Griffin, Acid-base and
244 tautomeric equilibria in the solid state: nitrogen-15 NMR spectroscopy of histidine and imidazole,
245 *J. Am. Chem. Soc.*, 1982, **104**, 1192–1196.
- 246 19 B. Henry, P. Tekely and J.-J. Delpuech, pH and pK Determinations by High-Resolution Solid-State ¹³C
247 NMR: Acid–Base and Tautomeric Equilibria of Lyophilized L-Histidine, *J. Am. Chem. Soc.*, 2002, **124**,
248 2025–2034.
- 249 20 S. P. Edgcomb and K. P. Murphy, Variability in the pKa of histidine side-chains correlates with burial
250 within proteins, *Proteins Struct. Funct. Bioinforma.*, 2002, **49**, 1–6.
- 251 21 C. Wang, R. A. Lamb and L. H. Pinto, Activation of the M2 ion channel of influenza virus: a role for the
252 transmembrane domain histidine residue, *Biophys. J.*, 1995, **69**, 1363–1371.
- 253 22 W. W. Cleland, Low-Barrier Hydrogen Bonds and Enzymatic Catalysis, *Arch. Biochem. Biophys.*, 2000,
254 **382**, 1–5.
- 255 23 E. F. Aziz, W. Eberhardt and S. Eisebitt, Effect of Cysteine vs. Histidine on the Electronic Structure of
256 Zn²⁺ Upon Complex Formation, *Z. Für Phys. Chem.*, 2008, **222**, 727–738.
- 257 24 A. Lampel, Biology-Inspired Supramolecular Peptide Systems, *Chem*, 2020, **6**, 1222–1236.
- 258 25 A. Levin, T. A. Hakala, L. Schnaider, G. J. L. Bernardes, E. Gazit and T. P. J. Knowles, Biomimetic
259 peptide self-assembly for functional materials, *Nat. Rev. Chem.*, 2020, **4**, 615–634.
- 260 26 W. Lu, E. Zhang, C. Amarasinghe, O. Kostko and M. Ahmed, Probing Self-Assembly in Arginine–Oleic
261 Acid Solutions with Terahertz Spectroscopy and X-ray Scattering, *J. Phys. Chem. Lett.*, 2020, **11**, 9507–
262 9514.
- 263 27 B. Gabryelczyk, H. Cai, X. Shi, Y. Sun, P. J. M. Swinkels, S. Salentinig, K. Pervushin and A. Miserez,
264 Hydrogen bond guidance and aromatic stacking drive liquid-liquid phase separation of intrinsically
265 disordered histidine-rich peptides, *Nat. Commun.*, 2019, **10**, 5465.
- 266 28 L. H. Al-Madhangi, S. K. Callear and S. L. M. Schroeder, Hydrophilic and hydrophobic interactions in
267 concentrated aqueous imidazole solutions: a neutron diffraction and total X-ray scattering study,
268 *Phys. Chem. Chem. Phys.*, 2020, **22**, 5105–5113.
- 269 29 B. M. Messer, C. D. Cappa, J. D. Smith, W. S. Drisdell, C. P. Schwartz, R. C. Cohen and R. J. Saykally,
270 Local Hydration Environments of Amino Acids and Dipeptides Studied by X-ray Spectroscopy of Liquid
271 Microjets, *J. Phys. Chem. B*, 2005, **109**, 21640–21646.
- 272 30 B. M. Messer, C. D. Cappa, J. D. Smith, K. R. Wilson, M. K. Gilles, R. C. Cohen and R. J. Saykally, pH
273 Dependence of the Electronic Structure of Glycine, *J. Phys. Chem. B*, 2005, **109**, 5375–5382.
- 274 31 J. Gråsjö, E. Andersson, J. Forsberg, L. Duda, E. Henke, W. Pokapanich, O. Björneholm, J. Andersson,
275 A. Pietzsch, F. Hennies and J.-E. Rubensson, Local Electronic Structure of Functional Groups in Glycine
276 As Anion, Zwitterion, and Cation in Aqueous Solution, *J. Phys. Chem. B*, 2009, **113**, 16002–16006.
- 277 32 M. Blum, M. Odellius, L. Weinhardt, S. Pookpanratana, M. Bär, Y. Zhang, O. Fuchs, W. Yang, E. Umbach
278 and C. Heske, Ultrafast Proton Dynamics in Aqueous Amino Acid Solutions Studied by Resonant
279 Inelastic Soft X-ray Scattering, *J. Phys. Chem. B*, 2012, **116**, 13757–13764.
- 280 33 F. Meyer, M. Blum, A. Benkert, D. Hauschild, S. Nagarajan, R. G. Wilks, J. Andersson, W. Yang, M.
281 Zharnikov, M. Bär, C. Heske, F. Reinert and L. Weinhardt, “Building Block Picture” of the Electronic
282 Structure of Aqueous Cysteine Derived from Resonant Inelastic Soft X-ray Scattering, *J. Phys. Chem. B*,
283 2014, **118**, 13142–13150.
- 284 34 M. Faubel, B. Steiner and J. P. Toennies, Photoelectron spectroscopy of liquid water, some alcohols,
285 and pure nonane in free micro jets, *J. Chem. Phys.*, 1997, **106**, 9013–9031.
- 286 35 D. Nolting, E. F. Aziz, N. Ottosson, M. Faubel, I. V. Hertel and B. Winter, pH-Induced Protonation of
287 Lysine in Aqueous Solution Causes Chemical Shifts in X-ray Photoelectron Spectroscopy, *J. Am. Chem.*
288 *Soc.*, 2007, **129**, 14068–14073.
- 289 36 N. Ottosson, K. J. Børve, D. Spångberg, H. Bergersen, L. J. Sæthre, M. Faubel, W. Pokapanich, G.
290 Öhrwall, O. Björneholm and B. Winter, On the Origins of Core–Electron Chemical Shifts of Small

- 291 Biomolecules in Aqueous Solution: Insights from Photoemission and ab Initio Calculations of
292 Glycineaq, *J. Am. Chem. Soc.*, 2011, **133**, 3120–3130.
- 293 37 D. Nolting, N. Ottosson, M. Faubel, I. V. Hertel and B. Winter, Pseudoequivalent Nitrogen Atoms in
294 Aqueous Imidazole Distinguished by Chemical Shifts in Photoelectron Spectroscopy, *J. Am. Chem.*
295 *Soc.*, 2008, **130**, 8150–8151.
- 296 38 B. Xu, M. I. Jacobs, O. Kostko and M. Ahmed, Guanidinium Group Remains Protonated in a Strongly
297 Basic Arginine Solution, *ChemPhysChem*, 2017, **18**, 1503–1506.
- 298 39 A. Barrozo, B. Xu, A. O. Gunina, M. I. Jacobs, K. Wilson, O. Kostko, M. Ahmed and A. I. Krylov, To Be or
299 Not To Be a Molecular Ion: The Role of the Solvent in Photoionization of Arginine, *J. Phys. Chem. Lett.*,
300 2019, **10**, 1860–1865.
- 301 40 J. G. Mesu, T. Visser, F. Soulimani and B. M. Weckhuysen, Infrared and Raman spectroscopic study of
302 pH-induced structural changes of l-histidine in aqueous environment, *Vib. Spectrosc.*, 2005, **39**, 114–
303 125.
- 304 41 V. Feyer, O. Plekan, N. Tsud, V. Cháb, V. Matolín and K. C. Prince, Adsorption of Histidine and
305 Histidine-Containing Peptides on Au(111), *Langmuir*, 2010, **26**, 8606–8613.
- 306 42 V. Feyer, O. Plekan, S. Ptasińska, M. Iakhnenko, N. Tsud and K. C. Prince, Adsorption of Histidine and a
307 Histidine Tripeptide on Au(111) and Au(110) from Acidic Solution, *J. Phys. Chem. C*, 2012, **116**, 22960–
308 22966.
- 309 43 Y. Zubavichus, A. Shaporenko, M. Grunze and M. Zharnikov, Innershell Absorption Spectroscopy of
310 Amino Acids at All Relevant Absorption Edges, *J. Phys. Chem. A*, 2005, **109**, 6998–7000.
- 311 44 V. Carravetta, O. Plashkevych and H. Ågren, A theoretical study of the near-edge x-ray absorption
312 spectra of some larger amino acids, *J. Chem. Phys.*, 1998, **109**, 1456–1464.
- 313 45 S. Eckert, J. Niskanen, R. M. Jay, P. S. Miedema, M. Fondell, B. Kennedy, W. Quevedo, M. Iannuzzi and
314 A. Föhlisch, Valence orbitals and local bond dynamics around N atoms of histidine under X-ray
315 irradiation, *Phys. Chem. Chem. Phys.*, 2017, **19**, 32091–32098.
- 316 46 O. Kostko, B. Xu, M. I. Jacobs and M. Ahmed, Soft X-ray spectroscopy of nanoparticles by velocity map
317 imaging, *J. Chem. Phys.*, 2017, **147**, 013931.
- 318 47 G. A. Garcia, L. Nahon and I. Powis, Two-dimensional charged particle image inversion using a polar
319 basis function expansion, *Rev. Sci. Instrum.*, 2004, **75**, 4989–4996.
- 320 48 M. J. Frisch, G. W. Trucks, H. B. Schlegel, G. E. Scuseria, M. A. Robb, J. R. Cheeseman, G. Scalmani, V.
321 Barone, B. Mennucci, G. A. Petersson, H. Nakatsuji, M. Caricato, X. Li, H. P. Hratchian, A. F. Izmaylov,
322 J. Bloino, G. Zheng, J. L. Sonnenberg, M. Hada, M. Ehara, K. Toyota, R. Fukuda, J. Hasegawa, M. Ishida,
323 T. Nakajima, Y. Honda, O. Kitao, H. Nakai, T. Vreven, J. A. Montgomery Jr., J. E. Peralta, F. Ogliaro, M.
324 J. Bearpark, J. Heyd, E. N. Brothers, K. N. Kudin, V. N. Staroverov, R. Kobayashi, J. Normand, K.
325 Raghavachari, A. P. Rendell, J. C. Burant, S. S. Iyengar, J. Tomasi, M. Cossi, N. Rega, N. J. Millam, M.
326 Klene, J. E. Knox, J. B. Cross, V. Bakken, C. Adamo, J. Jaramillo, R. Gomperts, R. E. Stratmann, O.
327 Yazyev, A. J. Austin, R. Cammi, C. Pomelli, J. W. Ochterski, R. L. Martin, K. Morokuma, V. G.
328 Zakrzewski, G. A. Voth, P. Salvador, J. J. Dannenberg, S. Dapprich, A. D. Daniels, Å. Farkas, J. B.
329 Foresman, J. V. Ortiz, J. Cioslowski and D. J. Fox, *Gaussian 09*, Gaussian, Inc., Wallingford, CT, USA,
330 2009.
- 331 49 S. Tardio and P. J. Cumpson, Practical estimation of XPS binding energies using widely available
332 quantum chemistry software, *Surf. Interface Anal.*, 2018, **50**, 5–12.
- 333 50 A. Sadybekov and A. I. Krylov, Coupled-cluster based approach for core-level states in condensed
334 phase: Theory and application to different protonated forms of aqueous glycine, *J. Chem. Phys.*,
335 2017, **147**, 014107.
- 336 51 J. M. Pi, M. Stella, N. K. Fernando, A. Y. Lam, A. Regoutz and L. E. Ratcliff, Predicting Core Level
337 Photoelectron Spectra of Amino Acids Using Density Functional Theory, *J. Phys. Chem. Lett.*, 2020, **11**,
338 2256–2262.

339

340 **Table 1:** Summary of all experimental C1s and N1s binding energies (in eV) for histidine aqueous aerosol
 341 generated at different pH conditions.

	C1s				N1s		
	carboxyl	amine, N=C-NH	C-N	C-C	amine	N=C-NH	N=C-NH
pH = 1	293.3	291.6	290.9	290.6	406.6	406.0	405.6
pH = 7	292.5	290.8	290.0	289.8	406.1	405.0	403.6
pH = 13	292.3	290.5	290.0	289.3	403.9	405.0	403.2

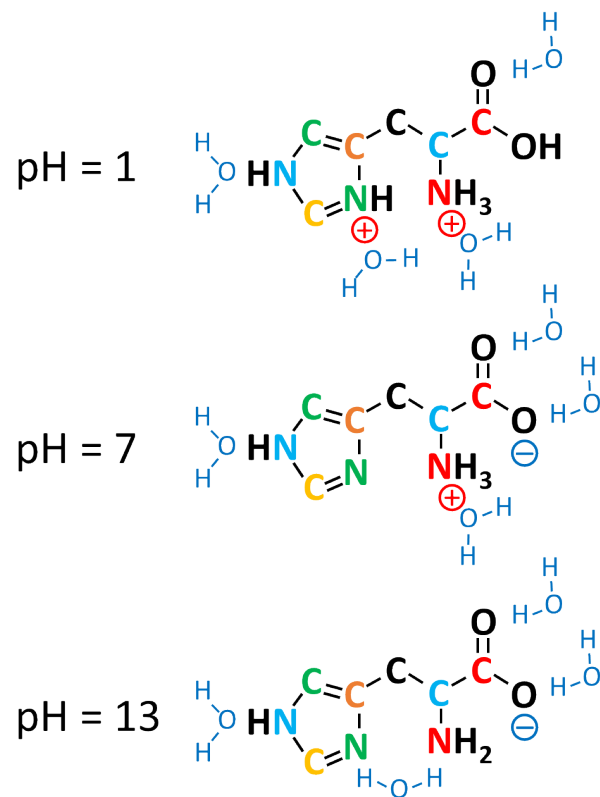
342

343

344 **Table 2:** Summary of all calculated C1s and N1s binding energies (in eV) for histidine aqueous aerosol
 345 generated at different pH conditions.

	C1s						N1s		
	carboxyl	amine	N=C-NH	C-NH	C-N	C-C	amine	N=C-NH	N=C-NH
pH = 1	294.4	292.4	292.5	291.2	291.5	290.8	407.5	406.3	406.3
pH = 7	292.2	290.9	290.9	290.0	290.0	289.8	405.9	405.1	403.6
pH = 13	291.7	289.8	290.8	289.9	289.8	289.2	402.8	405.0	403.5

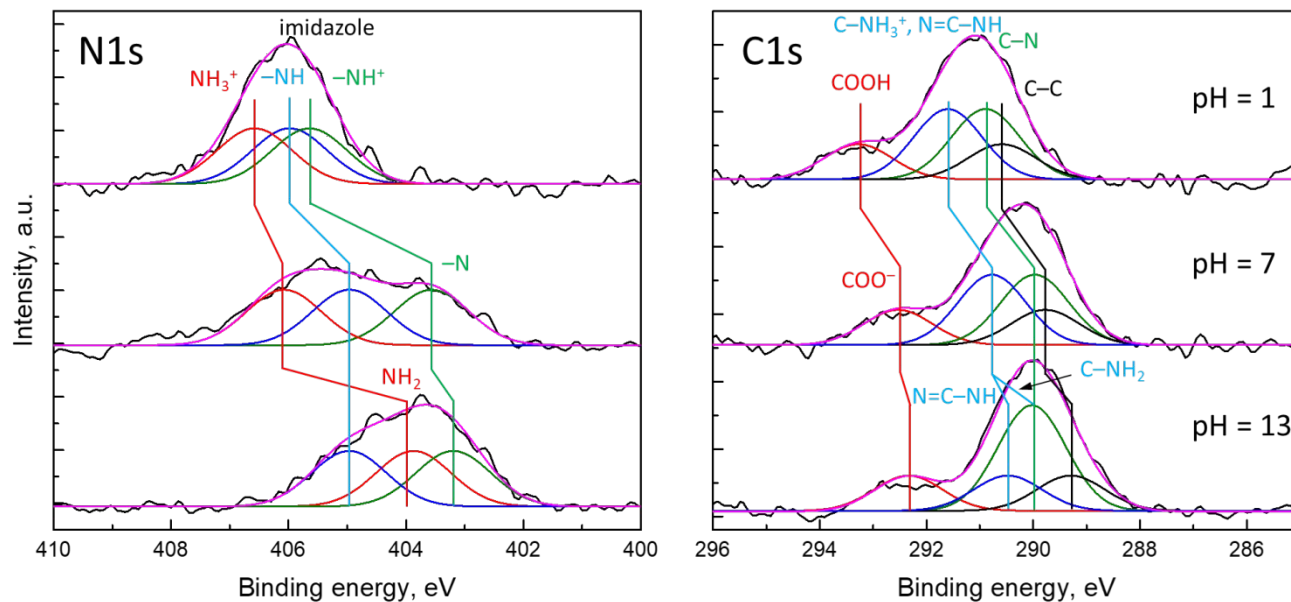
346



347

348 Figure 1. Dominating protonation forms of histidine in aqueous solution at different pH conditions.

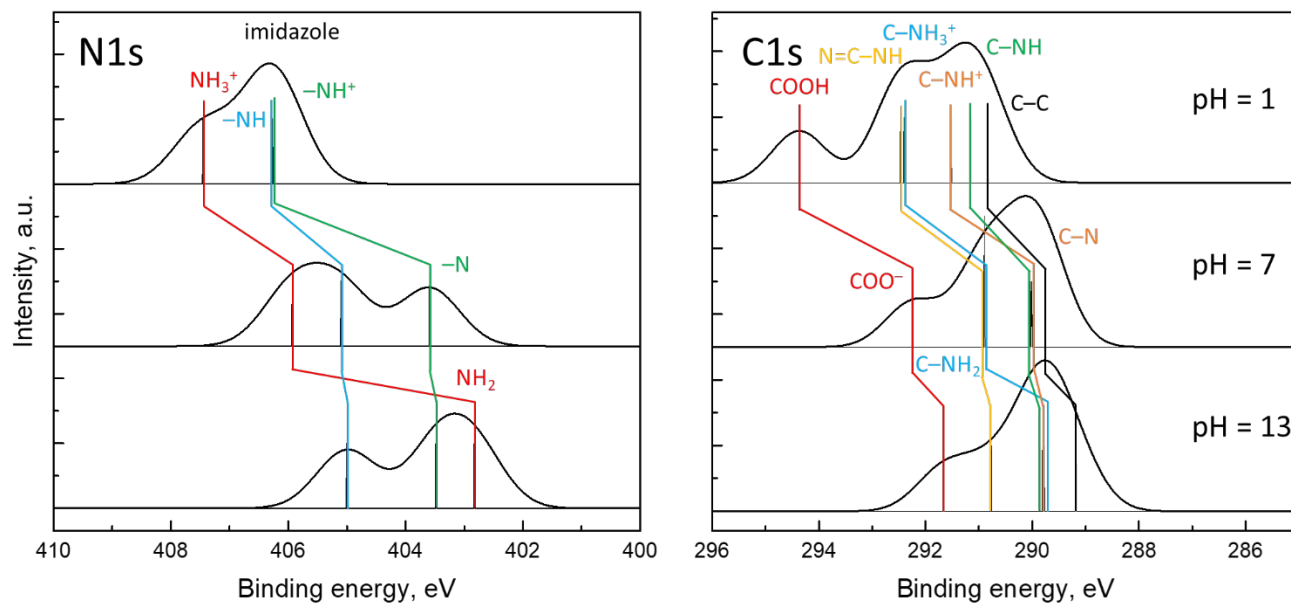
349



350

351 Figure 2. N1s and C1s photoelectron spectra of aqueous histidine collected at pH = 1 (top), pH = 7
 352 (middle), and pH = 13 (bottom). Black line represents experimental data, while magenta line represents
 353 total fit composed of sum of individual Gaussians (colored in red, blue, green, and black).

354



355

356 Figure 3. Theoretical N1s and C1s spectra of aqueous histidine collected at pH = 1 (top), pH = 7 (middle),
 357 and pH = 13 (bottom). Calculated binding energies are shown with vertical colored sticks. The spectrum
 358 is convoluted with Gaussian (FWHM = 1.2 eV) to correlate with the experimental photoelectron spectra
 359 and shown as black lines.